

Supporting Information for

**High-Fidelity Intracellular Imaging of Multiple miRNAs via
Stimulus-Responsive Nanocarriers and Catalytic Hairpin Assembly**

Hongyan Zhang^{a‡}, Wendong Liu^{a‡}, Fanghua Zhang^a, Zhihan Wu^a, Haijun Lu^a, Zhe Hao^a, Yu Liu^{a}, Xiyan Li^b, Ruizhong Zhang^a, Libing Zhang^{a*}*

^a Tianjin Key Laboratory of Molecular Optoelectronic Sciences, Department of Chemistry, Tianjin University, Tianjin 300072 P. R. China

^b Institute of Photoelectronic Thin Film Devices and Technology, Solar Energy Conversion Center, Key Laboratory of Photoelectronic Thin Film Devices and Technology of Tianjin, Engineering Research Center of Thin Film Photoelectronic Technology of Ministry of Education, Nankai University, Tianjin 300350 P. R. China

*Corresponding author.

‡ Contributed equally.

E-mail: tjly@tju.edu.cn (Y. L.); libing.zhang@tju.edu.cn (L.Z.)

Materials and methods

Chemicals and reagents.

All DNA oligonucleotides used in this experiment were purchased from Sangon Biotech Co., Ltd. (Shanghai, China) and purified by high-performance liquid chromatography (HPLC), and the sequences were listed in Tab. S1. Potassium permanganate (KMnO_4), oleic acid (OA), 4-(2-Hydroxyethyl) piperazine-1-ethanesulfonic acid sodium salt (HEPES), N, N, N', N'-Tetramethylethylenediamine (TEMED), N-Acetyl-L-cysteine (NAC), and N-ethylmaleimide (NEM) were purchased from Aladdin (Shanghai, China). Acryl/Bis 40% Solution (19:1), glutathione (GSH), TE buffer, 4S Red Plus nucleic acid stain, Deoxyribonuclease I (DNase I), Dulbecco's modified eagle medium (DMEM, high glucose), 3-(4,5-Dimethylthiazole)-2,5-diphenyltetrazolium bromide (MTT), DAPI stain solution, and Trypsin were purchased from Sangon Biotech Co., Ltd. (Shanghai, China). Magnesium chloride, sodium chloride, and ammonium persulfate (APS) were obtained from Macklin (Shanghai, China). CheKine™ Micro Reduced Glutathione (GSH) Assay Kit was bought from Abbkine Scientific Co., Ltd (Hubei, China).

Instrument.

Transmission electron microscopy (TEM) images and element mapping analysis were obtained on JEM-2100F (JEOL, Japan). The powder X-ray diffraction (PXRD) pattern of the material was obtained using X'Pert PRO MPD (PANalytical, Holland). X-ray photoelectron spectroscopy (XPS) measurement was performed on a K-Alpha X-ray photoelectron spectrometer (Thermo, America). The gel was imaged by Tanon 5200 (Tanon, China) under UV ($\lambda = 365 \text{ nm}$) irradiation. Fluorescence spectra were performed using an FS5 steady-state transient fluorescence spectrometer (Edinburgh, England). The zeta potential of the samples was measured on Zetasizer Nano ZS90 (Malvern, England). The Ultraviolet-visible (UV-vis) absorption spectra were collected on a UV-vis-NIR spectrophotometer (UV-3600 Plus, Shimadzu, Japan). Cell viability assay was measured on Infinite E Plex (Tecan, Austria). Confocal laser scanning microscopy (CLSM) imaging was carried out on a Nikon (A1R+, Japan) confocal microscope.

Synthesis of MnO_2 nanoparticle.

Firstly, 0.1g KMnO_4 was dissolved in 50 mL ultrapure water and stirred violently under room temperature for 1 h. Then, 1 mL OA was added and the mixture was continued to stir for another 24 h. The mauve solution is converted into a brown-black precipitate gradually. The sediment was collected and washed three times by

alternating centrifugation with anhydrous ethanol and ultrapure water, respectively. After that, the final product was acquired by drying the centrifuged product overnight in a vacuum drying oven at 70 °C.

Preparation of the Mn-CHP nanoprobe.

For the preparation of the Mn-CHP nanoprobe, 100 μ L MnO₂ (2 mg/mL) and 100 μ L four hairpin DNA in 10 mM HEPES buffer (100 mM NaCl, pH = 7.4) were mixed. After 40 min, the resulting mixture was diluted with HEPES to a final concentration of 200 μ g/mL MnO₂ and then incubated for another 20 min.

Fluorescence Detection of miRNA in vitro.

Four hairpin DNA (1 μ M, final concentration 100 nM) was mixed with different concentrations of miRNA-21 and miRNA-155. All assays were performed in 12.5 mM Tris-HCl buffer (100 mM NaCl, pH = 8.0) at 37 °C for 1 h.

Intracellular Imaging of miRNA.

Collect and culture 1×10^5 cells per dish at 37 °C overnight. The Mn-CHP probe (equivalent to 20 μ g/mL MnO₂) was incubated with the cells for 4 h. Then, remove the medium followed by washing cells with PBS three times. After that, the cells were fixed with 4% paraformaldehyde for 20 min and washed again with PBS. Finally, the nuclei were labeled with DAPI followed by washing with PBS. The fluorescence images were recorded on Nikon AR1⁺ confocal laser scanning microscopy (CLSM) under a 60 \times oil immersion objective.

Polyacrylamide Gel Electrophoresis.

12% Native polyacrylamide gel electrophoresis was employed to verify the feasibility of the strategy of catalytic hairpin assembly. Hairpin DNA (HP1, HP2 HP3, and HP4) in 20 mM Tris-HCl (100 mM NaCl, pH = 7.4) were annealed at 95 °C for 5 min and slowly cooled to room temperature for 2 h. Subsequently, HP1 and HP2 (HP3 and HP4) were incubated for 1 h at 37 °C in the absence or presence of miRNA-21 (miRNA-155). Then, 10 μ L of the samples (1 μ M) were mixed with 2 μ L 6 \times loading buffer and loaded into lanes of the pre-made gel which was prepared in 1 \times Tris-borate-EDTA (TBE) buffer. The gel was run in 1 \times TBE buffer at 110 V for 90 min and then stained for 30 min by Gel Red in the dark. Finally, the gel was imaged by a gel imager under UV light.

Test conditions for fluorescence emission spectroscopy.

The FAM-labeled probe was excited at 488 nm, and the fluorescence emission spectra were recorded between 510 nm and 600 nm. The cy5-labeled probe was excited at 638 nm and the fluorescence emission spectra were recorded between 660 nm and 710 nm.

Test conditions for confocal laser scanning microscopy.

The DAPI was excited under 405 nm and the fluorescence emission signals were recorded from 415 nm to 480 nm. The FAM-labeled probe was excited under 488 nm and the fluorescence emission signals were recorded from 515 nm to 580 nm. The Cy5-labeled probe was excited under 640 nm and the fluorescence emission signals were recorded from 665 nm to 715 nm.

Cell Culture.

The cell lines (MCF-7, HepG2, HeLa, and HEK293T) were cultured in DMEM supplemented with 10% FBS under 37 °C in a humid atmosphere containing 5% CO₂.

Cytotoxicity Assay.

The biocompatibility of the MnO₂ was evaluated via 3-(4,5-Dimethylthiazole)-2,5-diphenyltetrazolium bromide (MTT) assay. MCF-7 cells and HEK293T cells were seeded in 96-well plates and incubated at 37 °C before adding MnO₂. After 24 h, the cells were treated with different concentrations of MnO₂ (1, 5, 10, 15, 20, 30, 40, and 50 µg·mL⁻¹) for 12 h. Then, 1 µL penicillin-streptomycin and 10 µL MTT solution (5 mg/mL) were added to each well for 4 h. After that, 100 µL DMSO was added to replace the culture medium, and the absorption values were recorded under 490 nm.

Determination of intracellular GSH.

Before the assay, 2×10⁶ MCF-7 cells were seeded in a 6-well plate and incubated at 37 °C overnight. 200 µL NAC (400 µM), NEM (10 µM), and PBS were added and incubated with cells for 24 h (NAC and PBS) or 15 min (NEM), respectively. After, wash off the cells carefully and collect them by centrifugation (600 g, 10 min) with cold PBS twice. Next, 100 µL extraction buffer was added to each tube to resuspend the cells, and the cells were subjected to 2-3 freeze-thaw cycles using a -80 °C refrigerator. Finally, the supernatant was taken for further analysis after centrifugation (8000 g) for 10 min.

Flow cytometric analysis.

MCF-7, HeLa, HepG2 and HEK293T cells (1.0×10⁵ cells) were proceeded the same treatment mentioned in intracellular imaging of miRNA, then the cells were digested with 0.25% trypsin and centrifuged at 1000 rpm for 5 min, then washed with PBS for three times and redispersed in PBS for flow cytometry experiments.

Tab. S1. Sequence of the DNA used in this work.

Name	Sequence (5'-3')
HP1	FAM-TCAACATCAGTCTGATAAGCTACCTGTAGTACT AGCTTATCAGACTGA-BHQ1
HP2	ATAAGCTAGTACTACAGGTAGCTTATCAGACTGACCT GTAGTAC
HP3	Cy5-ACCCCTATCACGATTAGCATTAAACCATGTGTACT TAATGGTAATCGTGAT-BHQ3
HP4	ACCATTAAGTACACATGGTTAATGGTAATCGTGATCC ATGTGTAC
miRNA-21-D	TAGCTTATCAGACTGATGTTGA
miRNA-155-D	TTAATGCTAATCGTGATAGGGGT
Anti-21	TCAACATCAGTCTGATAAGCTA
Anti-155	ACCCCTATCACGATTAGCATTAA
miRNA-21	UAGCUUAUCAGACUGAUGUUGA
miRNA-155	UUAAUGGUAAUCGUGAUAGGGGU
Let-7a	UGAGGUAGUAGGUUGUAUAGUU
miRNA-144	UACAGUAUAGAUGAUGUACU
miRNA-122	UGGAGUGUGACAAUGGUGUUUG
miRNA-141	UAACACUGUCUGGUAAAGAUGG
miRNA-203	GUGAAAUGUUUAGGACCACUAG
Mis-21-1	UAGCUUAUCAGACUGAUG A UGA
Mis-155-1	UUAAUGGUAAUCGUGAUAG A GGU

The red bold letters represent the mismatched sites.

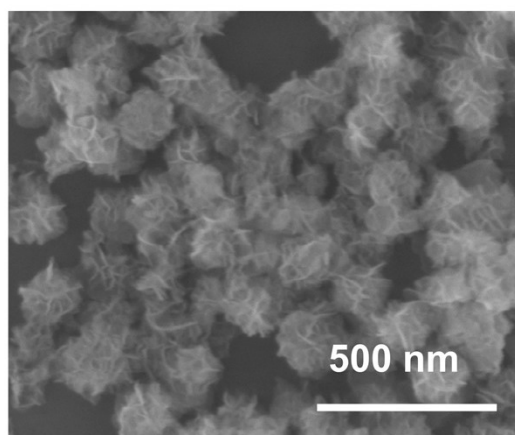


Fig. S1 Scanning electron microscopy image of MnO₂.

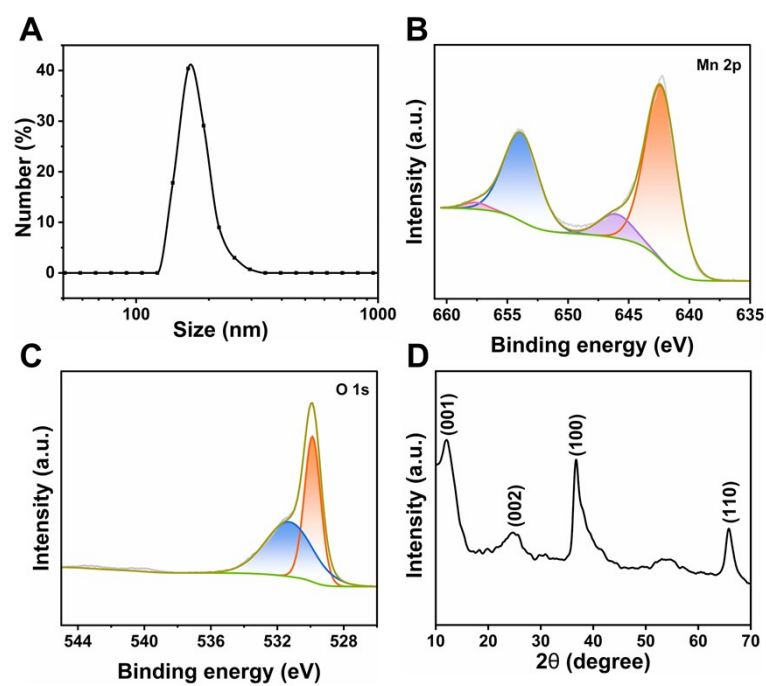


Fig. S2 (A) Hydrodynamic size of MnO₂. Mn 2p (B) and O 1s (C) of XPS spectra of MnO₂. (D) PXRD pattern of the MnO₂.

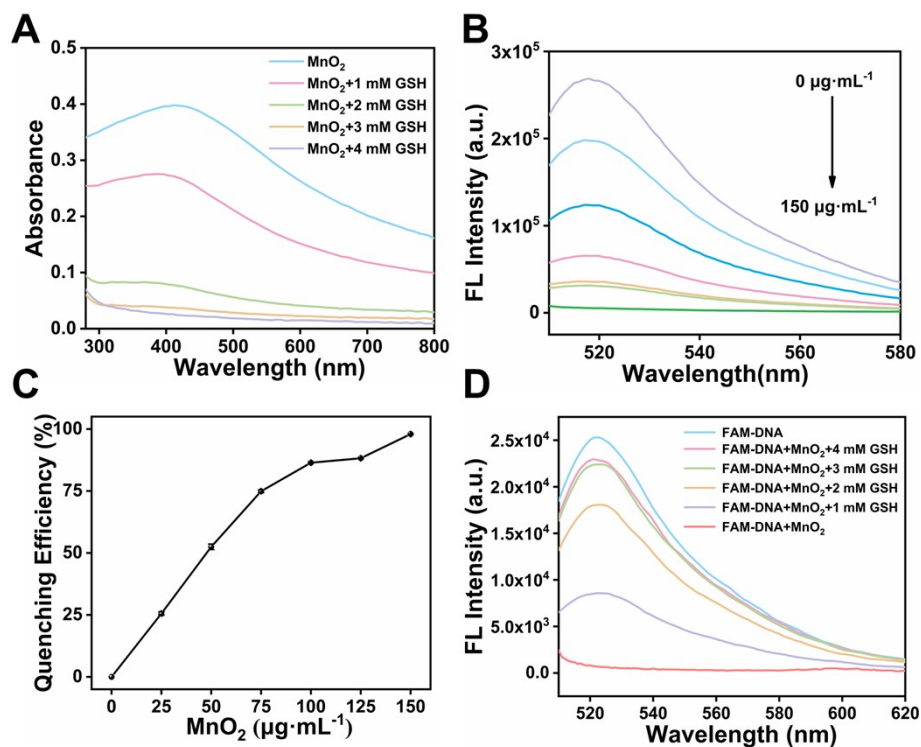


Fig. S3 (A) UV-Vis absorption spectra of the MnO₂ in the absence or the presence of different concentrations of GSH (1, 2, 3, 4 mM). (B) Fluorescence spectra of the FAM-DNA (100 nM) after incubating with different concentrations of MnO₂. (C) Quenching efficiency of MnO₂ after incubating with 200 nM FAM-DNA. The quenching efficiency was calculated by $[(F_0 - F)/F_0 \times C_{\text{FAM-DNA}}] / C_{\text{MnO}_2}$ (F_0 is the initial fluorescence response without MnO₂). The loading capacity of MnO₂ after incubating with 100 nM FAM-DNA was calculated by $(C_{\text{FAM-DNA}} \times \text{Quenching efficiency})/C_{\text{MnO}_2}$. (D) Fluorescence quenching and recovery of FAM-DNA with excitation wavelength at 488 nm for FAM.

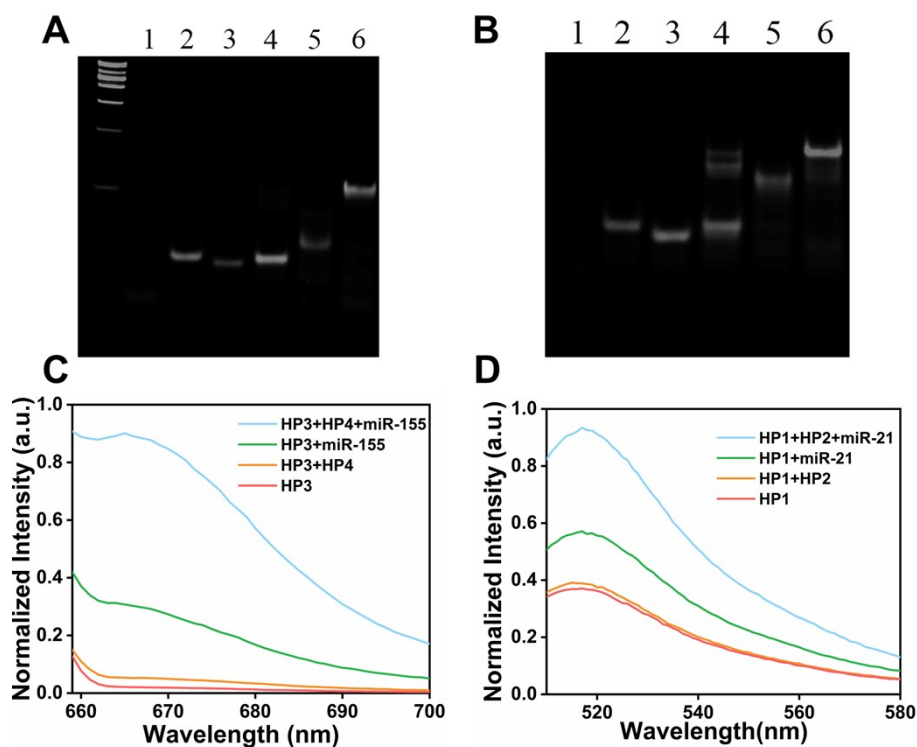


Fig. S4 (A) Gel electrophoresis images of the nanoprobe for miRNA-155 detection (lane 1: miRNA-155, lane 2: HP3, lane 3: HP4, lane 4: HP3+HP4, lane 5: miRNA-155+HP3, lane 6: miRNA-155+HP3+HP4). (B) Gel electrophoresis images of the nanoprobe for miRNA-21 detection (lane 1: miRNA-21, lane 2: HP1, lane 3: HP2, lane 4: HP1+HP2, lane 5: miRNA-21+HP1, lane 6: miRNA-21+HP1+HP2). Fluorescence spectra of the feasibility of nanoprobe for miRNA-155 (C) and miRNA-21 (D) detection.

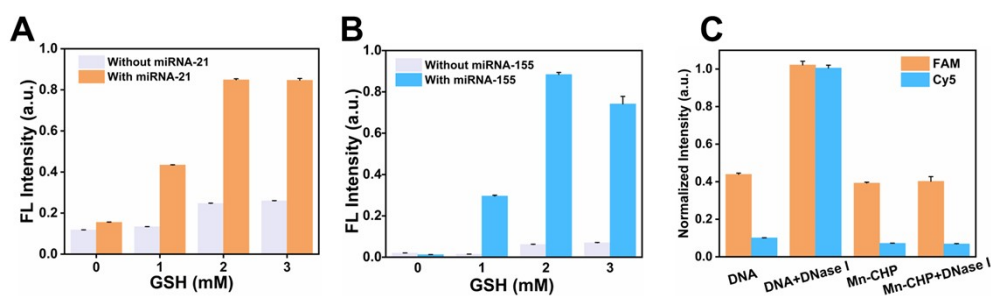


Fig. S5 Fluorescence intensity changes of Mn-CHP nanoprobe in response to different concentrations of GSH in the absence and presence of miRNA-21 (A) or miRNA-155 (B). (C) The fluorescence intensity of the bare CHA probes and the Mn-CHP nanoprobe in the absence or the presence of DNase I (FAM:520 nm, Cy5:667 nm). Error bars demonstrate the standard deviations of the results from three experiments.

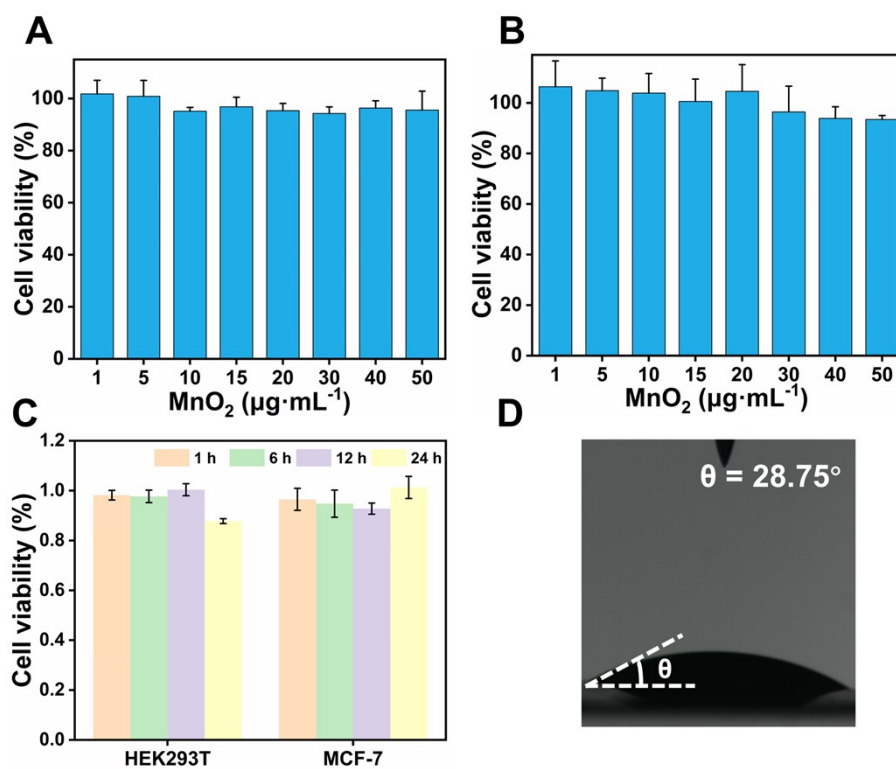


Fig. S6 Viabilities of MCF-7 (A) and HEK293T (B) cells treated with different concentrations of MnO₂ ranging from 1 to 50 µg·mL⁻¹. (C) Viabilities of HEK293T and MCF-7 cells treated with 20 µg·mL⁻¹ MnO₂ at different time points. (D) The water contact angle measurement of the MnO₂ nanoparticles.

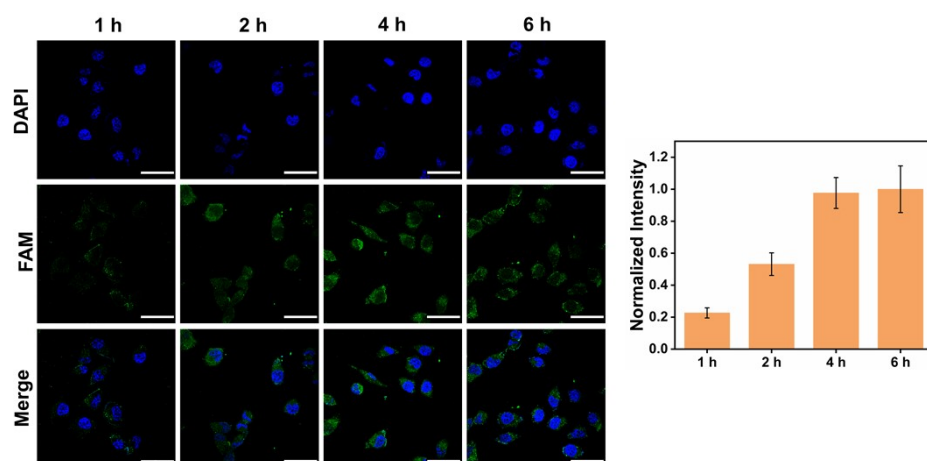


Fig. S7 The CLSM images of MCF-7 cells after incubating with the Mn-CHP probe for different times (1, 2, 4, 6 h). Scale bar: 50 μ m.

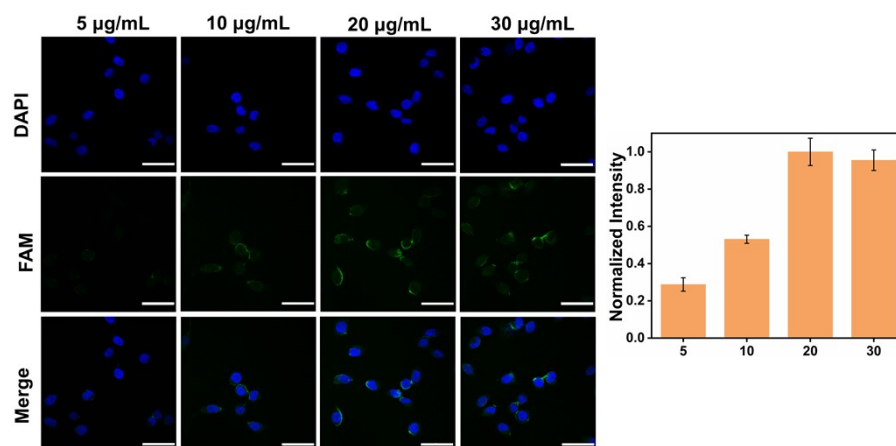


Fig. S8 The CLSM images of MCF-7 cells after incubating with the different concentrations of Mn-CHP probe (5, 10, 20, 30 $\mu\text{g/mL}$). Scale bar: 50 μm .

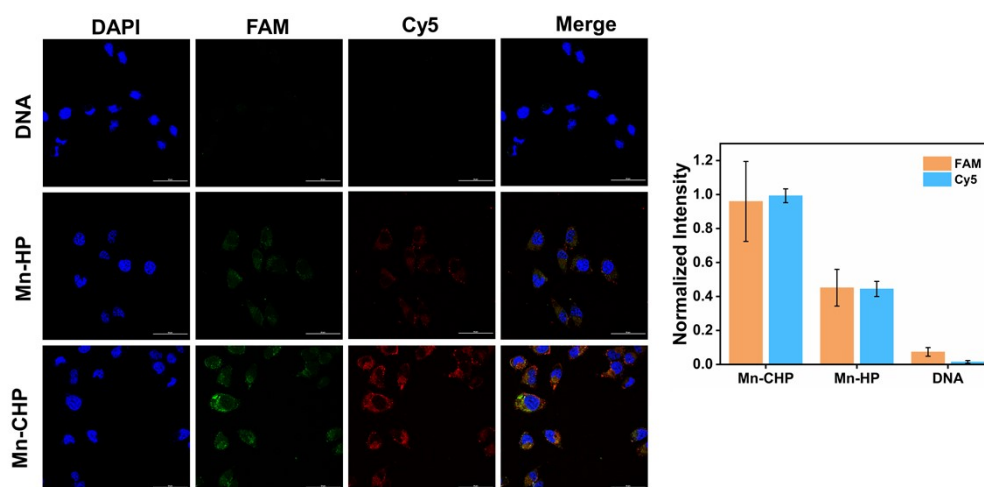


Fig. S9 The CLSM images of MCF-7 cells after incubating with the different nanoprobe for 4 h. Scale bar: 50 μ m.

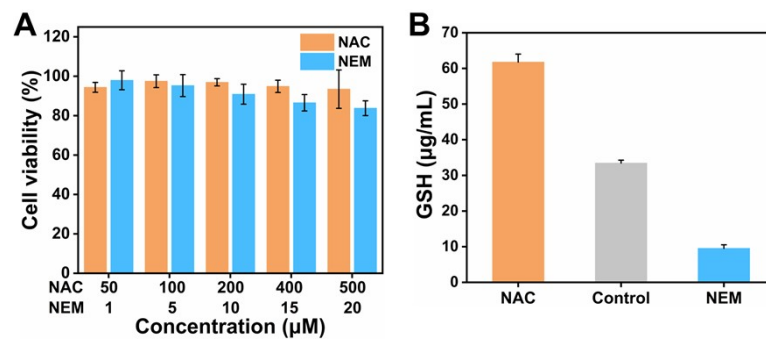


Fig. S10 (A) Cytotoxicity assays of NEM at different concentrations ranging from 1 to 20 µM (blue) and NAC at different concentrations ranging from 50 to 500 µM (orange). (B) Relative GSH level in living cells after treatment with NAC, culture medium (control), and NEM.

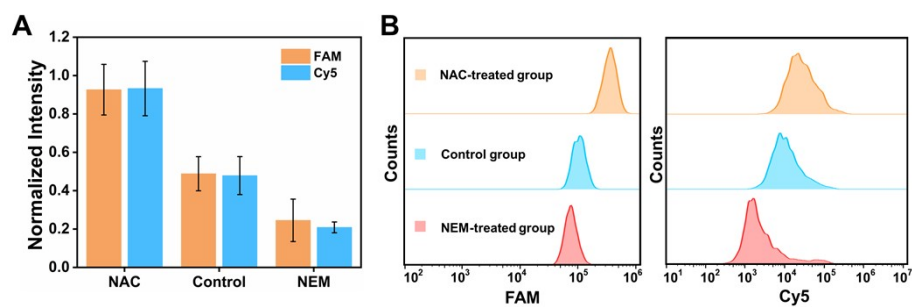


Fig. S11 (A) The corresponding fluorescence intensity analysis of CLSM images after treatment with NAC, culture medium (control), and NEM. Error bars demonstrate the standard deviations of the results from three experiments. (B) Flow cytometry analysis of MCF-7 cells that were treated with NAC, NEM, and culture medium (control), followed by Mn-CHP incubation.

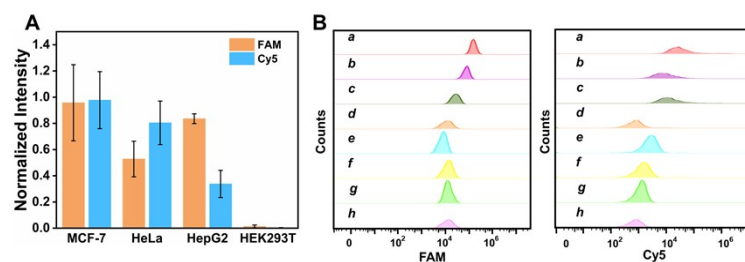


Fig. S12 (A) The corresponding fluorescence intensity analysis of CLSM images of different cell lines. (B) Flow cytometry analysis of MCF-7 cells (a for Mn-CHP and e for blank), HepG2 cells (b for Mn-CHP and f for blank), HeLa cells (c for Mn-CHP and g for blank) and HEK293T cells (d for Mn-CHP and h for blank).

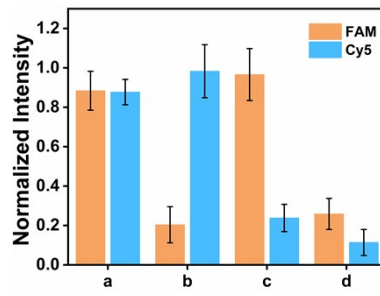


Fig. S13 The corresponding fluorescence intensity analysis of CLSM images after different treatments, a: control group, b: anti-21 group, c: anti-155 group, d: anti-21+anti-155 group.

Tab. S2. Comparison of the different sensors for intracellular miRNA analysis.

Method	Nanocarrier	Linear Range	Limit of Detection	Reference
Y-shaped DNA circuit	None	0.8-30 nM	450 pM	1
CHA on DNA tetrahedron	None	15-40 nM 5-20 nM	85 pM 26 pM	2
UiO-66-THMS	UiO-66-NH ₂	1-160 nM	400 pM	3
CHA-assisted DNA tetrahedron	None	0.1-10 nM	120 pM	4
CHA-assisted two-photon MOFs	UiO-66-NH ₂	1-60 nM	0.69 nM	5
Dual-mode AuNCs nanoplatform	GO	0-500 nM	0.91 nM	6
CHA-assisted Mn-CHP	MnO ₂	1-100 nM 1-100 nM	0.45 nM 0.47 nM	This work

Reference

1. C. Xie, R. Li, X. Gong, Q. Zhang, Y. Zhang, Z. Wang, X. Liu and F. Wang, *Anal. Chem.*, 2023, **95**, 10398-10404.
2. C. H. Li, W. Y. Lv, F. F. Yang, S. J. Zhen and C. Z. Huang, *ACS Appl. Mater. Interfaces*, 2022, **14**, 12059-12067.
3. Y. Han, R. Zou, L. Wang, C. Chen, H. Gong and C. Cai, *Talanta.*, 2021, **228**, 122199.
4. Q. Huang, P.-Q. Ma, H.-D. Li, B.-C. Yin and B.-C. Ye, *ACS Applied Bio Materials*, 2020, **3**, 2861-2866.
5. C. Yang, K. Wang, Z. Li, L. Mo and W. Lin, *Sens. Actuators B Chem.*, 2022, **359**, 131593.
6. B. Li, S. Yu, R. Feng, Z. Qian, K. He, G.-J. Mao, Y. Cao, K. Tang, N. Gan and Y.-X. Wu, *Anal. Chem.*, 2023, **95**, 14925-14933.